Published in final edited form as:
J Struct Biol. 2013 March ; 181(3): 264–273. doi:10.1016/j.jsb.2012.12.008.

Age-Related Nanostructural and Nanomechanical Changes of Individual Human Cartilage Aggrecan Monomers and Their Glycosaminoglycan Side Chains

Hsu-Yi Lee[a,1], **Lin Han**[b,c,1], **Peter Roughley**[d], **Alan J. Grodzinsky**[a,e,f,*], and **Christine Ortiz**[b,*]

[a]Department of Electrical Engineering and Computer Science, Massachusetts Institute of Technology, 77 Massachusetts Avenue, Cambridge, MA 02139

[b]Department of Materials Science and Engineering, Massachusetts Institute of Technology, 77 Massachusetts Avenue, Cambridge, MA 02139

[c]School of Biomedical Engineering, Science and Health Systems, Drexel University, 3141 Chestnut Street, Philadelphia, PA 19104

[d]Genetic Unit, Shriners Hospital for Children, McGill University, Montréal, QC H3G 1A6 Canada

[e]Department of Mechanical Engineering, Massachusetts Institute of Technology, 77 Massachusetts Avenue, Cambridge, MA 02139

[f]Department of Biological Engineering, Massachusetts Institute of Technology, 77 Massachusetts Avenue, Cambridge, MA 02139

Abstract

The nanostructure and nanomechanical properties of aggrecan monomers extracted and purified from human articular cartilage from donors of different ages (newborn, 29 and 38 year old) were directly visualized and quantified via atomic force microscopy(AFM)-based imaging and force spectroscopy. AFM imaging enabled direct comparison of full length monomers at different ages. The higher proportion of aggrecan fragments observed in adult versus newborn populations is consistent with the cumulative proteolysis of aggrecan known to occur in vivo. The decreased dimensions of adult full length aggrecan (including core protein and glycosaminoglycan (GAG) chain trace length, end-to-end distance and extension ratio) reflect altered aggrecan biosynthesis. The demonstrably shorter GAG chains observed in adult full length aggrecan monomers, compared to newborn monomers, also reflects markedly altered biosynthesis with age. Direct visualization of aggrecan subjected to chondroitinase and/or keratanase treatment revealed conformational properties of aggrecan monomers associated with chondroitin sulfate (CS) and keratan sulfate (KS) GAG chains. Furthermore, compressive stiffness of chemically end-attached layers of adult and newborn aggrecan was measured in various ionic strength aqueous solutions. Adult aggrecan was significantly weaker in compression than newborn aggrecan even at the same total GAG density and bath ionic strength, suggesting the importance of both electrostatic and non-electrostatic interactions in nanomechanical stiffness. These results provide molecular-level

*Correspondence and requests for materials should be addressed to: Christine Ortiz, Phone: 617-452-3084, Fax: 617-258-6936, cortiz@mit.edu, Alan J. Grodzinsky, Phone: 617-253-4969, Fax: 617-258-5239, alg@mit.edu.

[1]denotes equal contribution

evidence of the effects of age on the conformational and nanomechanical properties of aggrecan, with direct implications for the effects of aggrecan nanostructure on the age-dependence of cartilage tissue biomechanical and osmotic properties.

Keywords

cartilage; aggrecan; glycosaminoglycan; ultrastructure; aging

1. Introduction

Aggrecan, the most abundant proteoglycan in the extracellular matrix (ECM) of articular cartilage, is composed of a ~250 kDa core protein (Tortorella et al., 2002) substituted with ~100 chondroitin sulfate (CS) and ~30 keratan sulfate (KS) glycosaminoglycan (GAG) chains, as well as N-linked and O-linked oligosaccharides (Dudhia, 2005). In vivo, aggrecan monomers form high molecular weight aggregates (> 200 MDa) by noncovalently binding to hyaluronan (HA) stabilized by link protein (LP), which are enmeshed within a reinforcing collagen fibrillar network (Muir, 1979). This hierarchically structured ECM determines the unique biomechanical properties of cartilage, including load bearing and lubrication in synovial joints (Maroudas, 1979). Age and disease-induced deterioration of human cartilage (Hudelmaier et al., 2001) is characterized by significant structural heterogeneity of aggrecan, including differences in core protein and GAG side chain length, KS and CS substitution, and CS sulfate-ester substitution, which are critical determinants of cartilage charge density and distribution (Bayliss and Ali, 1978; Dudhia, 2005; Plaas et al., 2001; Plaas et al., 1997; Roughley and White, 1980). Progressive C-terminal truncation of the core protein by proteolytic enzymes takes place with increasing maturation (Sandy and Verscharen, 2001), and variations in aggrecan structure, in turn, can further affect its susceptibility to proteolytic digestions and development of osteoarthritis (Roughley et al., 2006).

Gel filtration chromatography and other biochemical assays have characterized age-related changes in the mean values of aggrecan and GAG molecular weight, composition and hydrodynamic size of large ensembles of cartilage-extracted aggrecan (Bayliss and Ali, 1978; Dudhia, 2005; Plaas et al., 2001; Plaas et al., 1997; Roughley and White, 1980). Such measures, however, cannot define the structure of *individual* aggrecan monomers, the degree of GAG variability within individual aggrecan, and the consequences of such ultrastructure on aggrecan molecular mechanics, all of which can regulate the macroscopic biomechanical and osmotic properties of articular cartilage as a function of age. This understanding could fill the knowledge gap between the conventional macroscopic tissue measurements and the underlying fundamental molecular-level properties of the matrix (Han et al., 2011; Hunziker et al., 2002; Stolz et al., 2007), issues of great importance to disease progression and tissue regeneration. High resolution imaging techniques, such as electron microscopy (Buckwalter and Rosenberg, 1982; Buckwalter and Rosenberg, 1983; Buckwalter et al., 1994; Morgelin et al., 1988; Rosenberg et al., 1975; Thyberg, 1977; Wiedemann et al., 1984) and atomic force microscopy (AFM) (Fritz et al., 1997; Jarchow et al., 2000; Todd et al., 2003), have shown the potential for examining aggrecan ultrastructure at the molecular level. We have recently demonstrated that high resolution AFM imaging can directly visualize and quantify the animal age and species-related variations in aggrecan ultrastructural features, such as the spatial distribution and length heterogeneity of GAG side chains (Kopesky et al., 2010; Lee et al., 2010; Ng et al., 2003). In addition, we have shown that AFM-based force spectroscopy can relate these structural features to aggrecan nanomechanical properties and their physical origins, such as ionic strength and [Ca^{2+}] dependence, and thereby provide

direct molecular evidence on the age-related changes in cartilage tissue functions (Dean et al., 2006; Han et al., 2007a; Han et al., 2007b; Han et al., 2008).

Toward this end, the goal of this study was to quantify age-related changes in the structure and nanomechanical properties of human aggrecan, and the role of CS- versus KS-GAGs in aggrecan conformation. Firstly, AFM-based high resolution imaging was utilized to quantify the structural and conformational parameters of individual aggrecan monomers extracted from newborn and adult human articular cartilage. The age-related differences in chondrocyte-mediated proteolytic and biosynthetic activities were distinguished for the first time via direct visualizing of individual monomers. Secondly, via selective removal of KS and/or CS GAG chains, we were able to distinguish the contributions of these GAG components to the molecular structure and stiffness of aggrecan. Thirdly, the compressive nanomechanical properties of aggrecan at different ages were evaluated via AFM-based force spectroscopy to correlate molecular mechanical behavior to the observed aggrecan nanostructures.

2. Materials and Methods

2.1 Isolation of human articular cartilage aggrecan

Macroscopically normal human articular cartilage samples were obtained at autopsy from the femoral condyles of one newborn, one 29 year-old and one 38 year-old adult with whom there was no evidence of arthritic disease or joint damage. Aggrecan was purified by dissociative CsCl density gradient centrifugation from 4 M guanidine HCl extracts of the cartilage, as described previously (Roughley and White, 1980). The initial dissociative (D1) fractions of the newborn and 38 year-old human samples were subjected to a second dissociative CsCl density gradient centrifugation, whereas part of the 29 year-old human initial D1 fractions was treated with keratanase II or chondroitinase ABC prior to the second dissociative density gradient centrifugation (see Section 2.2). The D1D1 fractions were then dialyzed exhaustively against water, lyophilized, dissolved in water, and stored at −20°C in 1 mg/ml aliquots.

2.2 Keratanase and chondroitinase treatments of human aggrecan

Part of the initial D1 fractions of the 29 year-old human aggrecan samples were treated with keratanase II or chondroitinase ABC in order to remove the KS- or CS-GAGs. The D1 fractions were first dissolved at 2 mg/ml in buffer. Aggrecan solution was then incubated at 37 °C for overnight with 5 mUnits keratanase II (Seikaguku, Tokyo, Japan) per mg aggrecan and 50 mM sodium acetate at pH 6.0 for KS-GAG removal, and 50 mUnits chondroitinase ABC (Seikagaku) per mg aggrecan, 100 mM Tris-HCl, 100 mM sodium acetate at pH 7.3 for CS-GAG removal. The digested samples were subsequently subjected to the second dissociative CsCl density gradient centrifugation, dialyzed, and stored at −20°C in 1 mg/ml aliquots.

2.3 AFM-based imaging and quantification of aggrecan structure

Aggrecan samples for AFM imaging were prepared following the procedures described previously (Ng et al., 2003). Briefly, 50 μl aggrecan aliquots (~100 μg/mL) were deposited on 3-aminopropyltriethoxysilane (APTES, Sigma Aldrich, St. Louis, MO) freshly treated muscovite mica surfaces (SPI Supplies, West Chester, PA, #1804 V-5) for 20–30 min at room temperature, rinsed gently with MilliQ water (18MΩ·cm resistivity, Purelab Plus UV/UF, US Filter, Lowell, MA) and air dried. Tapping mode AFM imaging was carried out in ambient conditions using rectangular Si AFM probe tips (AC240TS-2, Olympus, nominal spring constant $k = 2$ N/m, nominal tip radius $R < 10$ nm) and the Nanoscope IIIA

Multimode AFM (Veeco, Santa Barbara, CA). All imaging parameters were optimized to acquire high quality images.

The AFM height images were digitized into pixels and the aggrecan core protein structure features, including the trace lengths of core proteins L_{CP}, and the end-to-end distance, R_{ee}, were traced automatically with a custom Matlab (Mathworks) program (Kopesky et al., 2010). The trace lengths of the core protein, L_{CP}, and the end-to-end distance, R_{ee}, were calculated according to the spatial coordinates of the traces. The trace lengths of the GAG chains were traced manually with the SigmaScan Pro image analysis software (SPSS Science, Chicago, IL). The extension ratio, R_{ee}/L_{CP}, was calculated as a measure to demonstrate the degree of extension of each molecule. Nonparametric Mann-Whitney U-test was performed to test the difference of their mean values between each pair of populations without the assumption of normal distribution, with significance set at $p < 0.05$.

2.4 AFM-based nanomechanical test of aggrecan

Compressive nanomechanical properties of full length aggrecan were measured following the procedures described previously (Dean et al., 2005). In short, micropatterned surfaces with densely packed, chemically end-attached aggrecan and neutral, hydrophilic self-assembled monolayer (OH-SAM, 11-mercaptoundecanol, $HS(CH_2)_{11}OH$, Sigma Aldrich) were prepared via microcontact printing (Wilbur et al., 1994). A Multimode IV AFM with the PicoForce piezo (Veeco) was utilized to perform compressive nanomechanical tests with an OH-SAM functionalized, gold-coated spherical borosilicate colloidal probe tip (Novascan, Ames, IA , $k \sim 0.12$ N/m, $R \sim 2.5$ μm).

Two measurements were employed to assess the mechanical stiffness of the aggrecan at various ionic strengths. First, the compressed aggrecan layer height H was measured as a function of applied normal force via contact mode AFM scanning across the aggrecan-OH-SAM patterned surface at a given range of applied normal forces (0 ~ 30 nN) in NaCl aqueous solutions (ionic strength, IS = 0.001 to 1.0 M, pH ~ 5.6, tip lateral displacement rate = 60 μm/s). Secondly, aggrecan compression was performed by having the probe tip approach perpendicularly to the end-grafted aggrecan layer (z-piezo displacement velocity = 2 μm/s). The pH values of the aqueous solutions used in nanomechanical tests were measured to remain ~ 5.6 during the experiment (buffers were not used so that IS could be controlled down to 0.001 via NaCl alone). Raw data were converted to normal force as a function of tip-to-substrate distance, D, based on the height measurement (Dean et al., 2006). Normal stresses were calculated from the normal force using the surface element integration method (Bhattacharjee and Elimelech, 1997; Dean et al., 2006). The initial sulfated GAG (sGAG, including both CS-GAG and KS-GAG) density prior to compression as measured via the dimethylmethylene blue dye assay (Farndale et al., 1986), was ~ 20 mg/ml (one aggrecan molecule per 25 nm × 25 nm surface area) at 0.1 M NaCl for both newborn and adult cartilage aggrecan samples. sGAG density during compression was calculated as a function of compressed height by normalizing the total sGAG content under the probe tip to the reduced, compressed volume.

3. Results

3.1 Structural dimensions and heterogeneity of human aggrecan and constituent GAG chains

Structure and conformation of individual aggrecan monomers were directly visualized and the constituent GAG chains were clearly resolved in the AFM height images (Fig. 1). The globular domains at the core protein N- or C-terminals are distinct in these images (Fig. 1a and d, indicated by arrows). Aggrecan monomers consisting of globular domains at both

ends were defined as *full length aggrecan*. The characterization of the full-length aggrecan will be described in the following section.

In all the obtained images, newborn aggrecan were in general more uniform in size, whereas adult aggrecan exhibited greater variations in terms of L_{CP}. A greater portion of short fragments (~100 nm) bearing globular domains were also observed in the 29 and 38 year-old adult aggrecan populations (Fig. 1d,e). The short fragments are presumably the accumulated fragments from the proteolytic processing (Lark et al., 1997; Yasumoto et al., 2003).

The mean and 95% confidence interval of the aggrecan structural parameters L_{CP}, R_{ee} and Ree/L_{CP} for each population are reported in Table 1. These data suggest that the newborn population exhibits significantly larger values in all these parameters than either the 38 or 29 year old adult aggrecan populations ($p < 0.01$). In this study, we focused on the comparison between the newborn and 38 year old populations (Figs. 2), as the comparison with the 29 year old population yielded the same conclusions.

The CS GAG chain length L_{GAG} was found to be quite heterogeneous within one individual newborn and adult aggrecan monomer (Fig 3a), and the mean L_{GAG} of this individual newborn monomer was significantly greater than that of the adult monomer (Table 2, Fig 3a, $p < 0.0001$). These individual monomer L_{GAG} distributions were then compared to L_{GAG} for the entire populations of newborn and 38 year old aggrecan (Fig. 3b), as well as the identified full length monomers from these newborn and 38 year old aggrecan populations (Fig. 3c). The distributions and mean values of the individual, full length and all observed aggrecan populations were quite similar (Fig. 3), where GAG chains from the newborn aggrecan were significantly longer ($p < 0.0001$, Table 2).

3.2 Nanostructure of keratanase and chondroitinase treated aggrecan

The structural analysis of the 29 year old aggrecan population focused on the roles of KS- and CS-GAG chains on aggrecan structure and conformation. The keratanase II-treated aggrecan appeared globally similar to the untreated aggrecan (Fig. 4a–d), consistent with the presence of the many CS chains which are larger than KS. The chondroitinase ABC treated aggrecan had a relatively long, GAG-free region of core protein, corresponding to the position of the CS1 and CS2 domains, which occupy ~70% of the total aggrecan contour length (Fig. 4e–f). However, shorter GAG chains were still visible, located near the globular G1-G2 domains, corresponding to one of the putative locations of KS (Fig. 5).

Both KS- and CS-GAG removal resulted in significantly shorter L_{CP} for aggrecan with the full core proteins (Table 2 and Fig. 6a). Interestingly, the KS-removed aggrecan population showed values of R_{ee} and the extension ratio, R_{ee}/L_{CP}, similar to the those of the untreated population, both of which were significantly greater than the CS-removed population (Table 2 and Fig. 6b, c). The comparison of L_{CP} between full length and KS-removed aggrecan including all observed aggrecan populations resulted in no statistical difference, likely because the variations in L_{CP} introduced by the fragments overshadow the shortening effects of KS-removal on L_{CP}.

3.3 Compressive nanomechanics of full-length aggrecan under fully hydrated conditions

Aggrecan height, H, was measured as a function of applied normal force in electrolyte baths of 0.001 to 1.0 M NaCl. Consistent with previous observations on aggrecan from bovine and equine cartilage (Dean et al., 2006; Lee et al., 2010), H decreased monotonically with increasing applied normal force and ionic strength (Fig. 7a–d). The aggrecan heights measured at low forces reflect the relative differences in the lengths and the degree of extension of different aggrecan populations observed via AFM imaging (Fig. 7a,b). At all the tested ionic strengths, the newborn human aggrecan exhibited significantly greater

height than the 38-yr-old adult human aggrecan (Fig. 7a–d), consistent with the AFM imaging measurements on the distribution of L_{CP}, R_{ee} and R_{ee}/L_{CP} (Fig. 2b–d).

In the force spectroscopy measurements, normal forces were then measured as a function of the distance, D, between AFM probe tip and substrate. The normal force was found to increase nonlinearly with decreasing the tip-substrate separation distance, D (Fig. 7e, f), also consistent with previous observations (Dean et al., 2006; Lee et al., 2010). The newborn aggrecan also displayed longer range repulsive forces than the adult aggrecan at any given ionic strength, suggesting more superior compressive nanomechanical properties of newborn aggrecan molecules. The compressive behavior assessed via the height and force measurements coincide with each other, as shown for the measurements at 0.01 M ionic strength (Fig. 7g). The differences between H and D at small normal forces (< 5 nN) may be due to the tare force (~ 100 pN) necessary to enable stable feedback, and the additional weaker shear resistance of aggrecan during the contact mode height measurement (Han et al., 2007a).

The aggrecan compressive behavior of newborn and 38 year old aggrecan populations were directly compared at near-physiologic ionic strength, 0.10 M. The force-distance curves were converted to stress versus sGAG concentration (see Methods) (Fig. 8). The normal compressive resistance increased with increasing sGAG concentration for both populations; however, the newborn aggrecan exhibited a much stronger resistance to compressive stress than the adult aggrecan, even at the same sGAG concentration.

4. Discussion

In this study, direct visualization of individual human aggrecan molecules enabled separation of the proteolytic and biosynthetic variations in aggrecan ultrastructural and nanomechanical properties between age groups. Accumulated proteolytic activity, characterized by the increased heterogeneity and fragmentation of aggrecan was seen in both adult aggrecan populations. The variation in cell biosynthetic processes with age was reflected especially in the difference in GAG chain lengths, and to additional degrees by the full length aggrecan core protein length, end-to-end distance and extension ratio. In particular, the length of GAG side chains within single aggrecan molecules significantly decreased with age. In addition, the roles of various GAG side chain components were quantified by selective removal of KS-GAG and CS-GAG constituents. As a result of these structural changes, the uncompressed aggrecan volume (height) and compression resistance were also reduced in adult aggrecan populations.

4.1 Age-related aggrecan structural changes due to proteolytic variations

The progressive proteolytic modification of aggrecan during aging is evident in the presence of smaller aggrecan fragments in both newborn and adult aggrecan populations (Fig. 1). The adult aggrecan population contained markedly more fragmented aggrecan monomers (L_{CP} < 300 nm, Fig. 2a), showing the accumulation of enzymatically cleaved aggrecan with increasing age, e.g., monomers with partial CS-GAG domains or free G1-domains. In vivo, aggrecan core proteins are cleaved by a number of enzymes, primarily aggrecanases (a disintegrin and metalloproteinase with thrombospondin motifs, ADAMTS-4 and ADAMTS-5) and matrix metalloproteinases (MMPs) (Flannery et al., 1992; Sandy et al., 1991; Tortorella et al., 2002). Aggrecanases cleave aggrecan core protein in the interglobular domain (IGD) to produce free G1 domains (G1-NITEGE) (Sandy et al., 1991), and more efficiently (Tortorella et al., 2002) at distinctive sites within the CS region to leave fragments with partially retained GAG chains and core protein lengths ~ 25 – 75% of the full length aggrecan. MMPs can cleave the core protein in the IGD (Flannery et al., 1992) to produce another type of free G1 domain (G1-VDIPEN). These proteolytic activities are

directly reflected in the observed high concentration of aggrecan fragments with reduced L_{CP} within the adult population (Fig. 2a). While G1-free fragments are expected to diffuse out of cartilage after cleavage, G1-associated fragments retain the capability of binding to hyaluronan. Thus, these fragments are known to accumulate in cartilage tissue with age (Lark et al., 1997; Yasumoto et al., 2003). Compared to intact aggrecan with a half-life of ~ 3.5 years in the inter-territorial matrix, the free-G1 domains have a much longer resident time in the matrix of 19 – 25 years (Maroudas et al., 1998; Verzijl et al., 2001). The accumulation of free G1-domains has been hypothesized to be detrimental to cartilage, as they can worsen biomechanical properties by competing with full length aggrecan on the hyaluronan binding sites (Mercuri et al., 1999).

The accumulation of proteolytically-derived aggrecan fragments is diminished for the newborn aggrecan, reflected by the greater values of average L_{CP} (Fig. 2a), and smaller difference with its full aggrecan subpopulation (Fig. 2b). This aggrecan structure comparison thus provided direct observation on the cumulative age-related proteolytic effects on cartilage aggrecan heterogeneity and polydispersity at the individual molecular level. In vivo, the differences of cartilage aggrecan polydispersity between these two age groups are expected to be more pronounced than the observation here (Figs. 1 and 2), as the density-based D1D1 sample preparation procedure has removed a large portion of GAG-deplete aggrecan fragments (Roughley and White, 1980), and thus, reduced the polydispersity to a larger extent in the adult aggrecan population (Bayliss and Ali, 1978; Dudhia et al., 1996; Plaas et al., 2001; Roughley and White, 1980).

4.2 Age-related aggrecan core protein structural changes due to biosynthesis variations

With the advantages of direct visualization, we were able to specifically pick the full length aggrecan subpopulation, which had globular domains identified at both the N- and C-termini (Fig. 1c, f). The full length aggrecan monomers have not undergone enzymatic modifications and, hence, only reflect the results of chondrocyte biosynthetic processes. Moreover, the metabolic half life of full length aggrecan is ~ 3.4 years (Maroudas et al., 1998), shorter than the age difference between the newborn and adult (both 29 and 38 year old) human subjects. Hence, the full length aggrecan found in the adult populations are most likely synthesized later in the subject's life time. In the absence of proteolytic modifications, the significantly greater values of full length aggrecan core protein trace length, L_{CP}, provide direct evidence of the age-related variations in the chondrocyte biosynthetic activities. It is likely that this age-related decrease in core protein length is not a direct result of variation in core protein synthesis, but rather an indirect consequence of variations in the sulfation pattern, number and length of GAG side chains (Dudhia, 2005; Roughley and White, 1980).

4.3 Age-related glycosaminoglycan chain structural changes due to biosynthesis variations

Although previous chromatography (Carney et al., 1985; Deutsch et al., 1995; Inerot et al., 1978; Plaas et al., 1997) and electron microscopy (Buckwalter et al., 1994) studies have suggested significant shortening of GAG chain lengths with increasing age, this study for the first time provided detailed ultrastructural characterization and comparison of GAGs attached to human aggrecan based on the information from individual molecules (Fig. 3). Within each individual full length aggrecan (Fig. 1c, f), GAG chains of the adult aggrecan are considerably shorter than those of newborn aggrecan (Fig. 3a).

For the newborn population, most of the GAG chains are CS-GAGs, whereas for the adult population, the observed GAG chains are likely a mixture of CS- and KS-GAGs. The differences in both chain lengths (Brown et al., 1998; Huckerby et al., 1999; Santer et al.,

1982) and number of chains (Elliott and Gardner, 1979) between KS and CS decrease with age. The narrower distribution of L_{GAG} seen in the individual adult aggrecan monomers (Fig. 3a) may also reflect the decreased GAG length heterogeneity due to the decreased length differences between CS and KS with age (Brown et al., 1998; Huckerby et al., 1999; Santer et al., 1982), or between CS chains in the CS1 and CS2 regions (Rodriguez et al., 2006).

4.4 Age-related variations in aggrecan conformation and compressive nanomechanical properties

The end-to-end distance, R_{ee}, and extension ratio, R_{ee}/L_{CP}, of the newborn aggrecan are markedly greater than the adult population (Fig. 2c, d). Newborn human aggrecan molecules thus adapt a more extended conformation compared to the adult aggrecan, owing to the stronger steric and electrostatic repulsion as a result of longer GAG chains and greater net charge densities. The conformational entropic effects are less important, leading to a more extended, less coil-like molecular conformation (Flory, 1953). Similarly, due to the stronger GAG-GAG repulsion, the newborn population also demonstrates greater initial height and higher compressive stiffness compared to the adult aggrecan upon compression nanomechanical test at physiological-like conditions (Fig. 7). The higher electrostatic forces for the newborn population arise from the greater number of charges per GAG chain, greater number of GAG chains, and possibly smaller GAG-GAG molecule spacing along the core protein. The higher nonelectrostatic forces are related to the larger dimensions of aggrecan (i.e, L_{CP} and L_{GAG}). Macroscopically, the compressive modulus of cartilage correlates well with GAG fixed charge density (Williamson et al., 2001). At the nanoscale, we have shown that the molecular structure and dimension of aggrecan and GAGs also affect the compressive behavior of aggrecan (Dean et al., 2006; Lee et al., 2010). At physiologic-like ionic strength (0.10 M), higher compressive stress was observed for the newborn aggrecan than the adult aggrecan even at the same sulfated GAG (sGAG) density (Fig. 8). This difference is due to the larger nonelectrostatic (steric and entropic) components (Bathe et al., 2005; Comper and Laurent, 1978), as well as variation in the heterogeneity of charge and electrostatic potential distributions within the end-grafted aggrecan layer (Buschmann and Grodzinsky, 1995; Dean et al., 2003). This difference further demonstrates the importance of aggrecan molecular architecture and associated heterogeneous, spatially nonuniform charge distribution in determining aggrecan molecular mechanics and cartilage tissue stiffness.

4.5 Structure and distribution of different GAG side chain components

Using the 29-year-old human aggrecan population as the model system, we directly identified the spatial distribution of different KS- and CS-GAG side chain components along the aggrecan core protein, and explored and identified their contributions to the structure and properties of aggrecan by selective removal of each constituent (Fig. 4). The KS-GAGs only make up a small fraction of the side chains, as removal of KS-GAGs did not lead to marked changes in the brush-like aggrecan structure (Fig. 4d). On the other hand, the majority of the GAGs are CS-GAG chains, where removal of CS-GAGs essentially transforms aggrecan into a linear core protein, with only traces of shorter KS-GAGs near the N-terminal (Figs. 4f and 5). This observation thus provides the direct experimental evidence that supports the previous hypothesis on the structure and spatial distribution of aggrecan side chain constituents (Hardingham and Fosang, 1992; Ng et al., 2003).

4.6 Contribution of GAG side chains to aggrecan conformation

Removal of both KS-GAG and CS-GAG significantly reduced the core protein trace length, L_{CP} (Fig. 6a). Because neither keratanase II nor chondroitinase ABC modifies the amino acid sequence and physical contour length of the core protein (Oike et al., 1980), the

decrease in the trace length, L_{CP}, can be attributed to a less extended short range conformation of the core protein, and the local coiling and aggregation of amino acid units due to hydrophobic interactions or electrostatic attraction. These short range conformation changes can take place at the length scale beyond the resolution of AFM imaging (~ 2 nm), and thus, result in reduced measured values of L_{CP}. This effect is more pronounced for the CS-removed aggrecan, given the presence of strikingly more CS-GAGs than KS-GAGs within each aggrecan.

Interestingly, removal of KS-GAG chains had negligible effects on the distribution of the end-to-end distance, R_{ee}, or the extension ratio, R_{ee}/L_{CP} (Fig. 6b, c). This observation suggests that the KS-GAG constituents play minor roles in determining aggrecan molecular conformation and deformation, given the small number of KS-GAGs, the shorter chain lengths and much smaller number of negative charges compared to CS-GAGs. By comparison, removal of CS-GAG chains led to significant decreases in R_{ee} and R_{ee}/L_{CP} (Fig. 6b, c). Since CS-GAGs contribute to most of the negative charges of aggrecan, CS-GAG-absent aggrecan behaves more similarly to linear protein molecules, with only traces of shorter GAG chains visible near one end of the core protein, presumably the KS-GAG chains close to the N-terminal (Fig. 5). These few short KS-GAG chains thus have minimal impact on the intra-molecular steric, electrostatic repulsion, and nanomechanical properties of aggrecan, consistent with the observation that the KS-removed aggrecan behave similar to the full length aggrecan (Fig. 6).

4.7 Implications regarding age-related cartilage tissue degradation and repair

Age-related weakening of aggrecan is known to be directly related to function changes in articular cartilage. Decreases in cartilage modulus and increases in hydraulic permeability of cartilages with age may be attributed to the weaker molecular stiffness of full length aggrecan (Figs. 4 and 5), as well as the higher concentration of enzymatically cleaved G1-associated fragments that are bound to hyaluronan. In addition, in vivo, aggrecan molecules are entrapped within the collagen fibrillar network in a pre-strained state, with molecular strains ~ 40 – 60% for macroscopically uncompressed cartilage (Wight et al., 1991). Under these finite molecular strains, differences in compressive resistance between the newborn and adult aggrecan at the same GAG concentration are even more prominent (Fig. 8). These results give direct experimental evidence of progressive changes in human cartilage properties that may result from changes at the molecular-level, further elucidating the relation between aggrecan monomer structure and biomechanical properties of cartilage.

Interestingly, the biosynthesis-related structural and mechanical differences observed here between the extracted newborn versus adult aggrecan are similar to the differences observed with aggrecan synthesized by adult equine bone marrow stromal cells (BMSCs) versus chondrocytes from the same animals (Lee et al., 2010). The BMSC-synthesized aggrecan monomers show nanostructural and nanomechanical properties superior to the aggrecan synthesized by adult equine chondrocytes, largely due to differences in GAG chain length. Consequently, BMSC-aggrecan also exhibits higher compressive stresses than adult cartilage aggrecan at the same sGAG concentration (Kopesky et al., 2010; Lee et al., 2010).

5. Conclusions

In this study, the age-related structure and property changes of aggrecan monomers from human articular cartilage were quantified at the length scales of individual molecules and physiological-like molecular assemblies. While previous biochemical studies have reported age-related changes in large ensembles of human cartilage aggrecan, this study provides direct evidence of the modifications by proteolytic and biosynthetic processes on the structure, conformation and mechanical behavior of aggrecan related to individual

molecules. These molecular-level changes, including accumulation of fragmented aggrecan, reduction in aggrecan and CS-GAG size (L_{CP}, L_{GAG}), changes in conformation (R_{ee}, R_{ee}/L_{CP}), and decrease in aggrecan compressive stiffness are characteristics of cartilage aging in vivo, and directly affect the tissue function of cartilage and the risk of osteoarthritis. AFM-based direct visualization of individual aggrecan has enabled us to separate the full-length and fragmented aggrecan populations, and therefore de-convolute the effects of changes in proteolytic cleavage and chondrocyte biosynthesis mechanisms. In addition, the roles of CS-GAG and KS-GAG side chains on aggrecan conformation were distinguished via this direct visualization method. This study provides the knowledge basis to link certain age- and osteoarthritis-related changes in cartilage tissue to fundamental molecular processes that take place at the nanometer length scale. It is hoped that the information presented here will aid further progress in the field of osteoarthritis research, including detecting early-stage disease, documenting the disease progression, as well as assessing and optimizing treatment interventions.

Acknowledgments

This work was supported by the National Science Foundation (grant CMMI-0758651), the National Institutes of Health (grant AR33236), the National Security Science and Engineering Faculty Fellowship (grant N00244-09-1-0064), and the Shriners of North America. The authors thank the Institute for Soldier Nanotechnologies at MIT, funded through the U.S. Army Research Office, for the use of instruments.

References

Bathe M, Rutledge GC, Grodzinsky AJ, Tidor B. A coarse-grained molecular model for glycosaminoglycans: application to chondroitin, chondroitin sulfate, and hyaluronic acid. Biophys. J. 2005; 88:3870–3887. [PubMed: 15805173]

Bayliss MT, Ali SY. Age-related changes in the composition and structure of human articular-cartilage proteoglycans. Biochem. J. 1978; 176:683–693. [PubMed: 747646]

Bhattacharjee S, Elimelech M. Surface element Integration: a novel technique for evaluation of DLVO interaction between a particle and a flat plate. J. Colloid Interface Sci. 1997; 193:273–285. [PubMed: 9344528]

Brown GM, Huckerby TN, Bayliss MT, Nieduszynski IA. Human aggrecan keratan sulfate undergoes structural changes during adolescent development. J. Biol. Chem. 1998; 273:26408–26414. [PubMed: 9756873]

Buckwalter JA, Rosenberg LC. Electron microscopic studies of cartilage proteoglycans. Direct evidence for the variable length of the chondroitin sulfate-rich region of proteoglycan subunit core protein. J. Biol. Chem. 1982; 257:9830–9839. [PubMed: 6809744]

Buckwalter JA, Rosenberg LC. Structural changes during development in bovine fetal epiphyseal cartilage. Collagen Rel. Res. 1983; 3:489–504.

Buckwalter JA, Roughley PJ, Rosenberg LC. Age-related changes in cartilage proteoglycans: quantitative electron microscopic studies. Microsc. Res. Tech. 1994; 28:398–408. [PubMed: 7919527]

Buschmann MD, Grodzinsky AJ. A molecular model of proteoglycan-associated electrostatic forces in cartilage mechanics. J. Biomech. Eng. 1995; 117:179–192. [PubMed: 7666655]

Carney SL, Billingham MEJ, Muir H, Sandy JD. Structure of newly synthesized (^{35}S)-proteoglycans and (^{35}S)-proteoglycan turnover products of cartilage explant cultures from dogs with experimental osteoarthritis. J. Orthop. Res. 1985; 3:140–147. [PubMed: 3998892]

Comper WD, Laurent TC. Physiological function of connective tissue polysaccharides. Physiol. Rev. 1978; 58:255–315. [PubMed: 414242]

Dean D, Seog J, Ortiz C, Grodzinsky AJ. Molecular-level theoretical model for electrostatic interactions within polyelectrolyte brushes: applications to charged glycosaminoglycans. Langmuir. 2003; 19:5526–5539.

Dean D, Han L, Ortiz C, Grodzinsky AJ. Nanoscale conformation and compressibility of cartilage aggrecan using microcontact printing and atomic force microscopy. Macromolecules. 2005; 38:4047–4049.

Dean D, Han L, Grodzinsky AJ, Ortiz C. Compressive nanomechanics of opposing aggrecan macromolecules. J. Biomech. 2006; 39:2555–2565. [PubMed: 16289077]

Deutsch AJ, Midura RJ, Plaas AHK. Structure of chondroitin sulfate on aggrecan isolated from bovine tibial and costochondral growth plates. J. Orthop. Res. 1995; 13:230–239. [PubMed: 7722760]

Dudhia J. Aggrecan, aging and assembly in articular cartilage. Cell. Mol. Life Sci. 2005; 62:2241–2256. [PubMed: 16143826]

Dudhia J, Davidson CM, Wells TM, Vynios DH, Hardingham TE, Bayliss MT. Age-related changes in the content of the C-terminal region of aggrecan in human articular cartilage. Biochem. J. 1996; 313:933–940. [PubMed: 8611178]

Elliott RJ, Gardner DL. Changes with age in the glycosaminoglycans of human articular cartilage. Ann. Rheum. Dis. 1979; 38:371–377. [PubMed: 496451]

Farndale RW, Buttle DJ, Barrett AJ. Improved quantitation and discrimination of sulphated glycosaminoglycans by use of dimethylmethylene blue. Biochim. Biophys. Acta. 1986; 883:173–177. [PubMed: 3091074]

Flannery CR, Lark MW, Sandy JD. Identification of a stromelysin cleavage site within the interglobular domain of human aggrecan. Evidence for proteolysis at this site in vivo in human articular cartilage. J. Biol. Chem. 1992; 267:1008–1014. [PubMed: 1730630]

Flory, PJ. Ithaca: Principles of Polymer Chemistry Cornell Univ. Press; 1953.

Fritz J, Anselmetti D, Jarchow J, Fernàndez-Busquets X. Probing single biomolecules with atomic force microscopy. J. Struct. Biol. 1997; 119:165–171. [PubMed: 9245757]

Han L, Grodzinsky AJ, Ortiz C. Nanomechanics of the cartilage extracellular matrix. Annu. Rev. Mater. Res. 2011; 41:133–168. [PubMed: 22792042]

Han L, Dean D, Ortiz C, Grodzinsky AJ. Lateral nanomechanics of cartilage aggrecan macromolecules. Biophys. J. 2007a; 92:1384–1398. [PubMed: 17142289]

Han L, Dean D, Mao P, Ortiz C, Grodzinsky AJ. Nanoscale shear deformation mechanisms of opposing cartilage aggrecan macromolecules. Biophys. J. 2007b; 93:L23–L25. [PubMed: 17586571]

Han L, Dean D, Daher LA, Grodzinsky AJ, Ortiz C. Cartilage aggrecan can undergo self-adhesion. Biophys. J. 2008; 95:4862–4870. [PubMed: 18676640]

Hardingham TE, Fosang AJ. Proteoglycans: many forms and many functions. FASEB J. 1992; 6:861–870. [PubMed: 1740236]

Huckerby TN, Nieduszynski IA, Bayliss MT, Brown GM. 600 MHz NMR studies of human articular cartilage keratan sulfates. Eur. J. Biochem. 1999; 266:1174–1183. [PubMed: 10583415]

Hudelmaier M, Glaser C, Hohe J, Englmeier KH, Reiser M, Putz R, Eckstein F. Age-related changes in the morphology and deformational behavior of knee joint cartilage. Arthritis Rheum. 2001; 44:2556–2561. [PubMed: 11710712]

Hunziker PR, Stolz M, Aebi U. Nanotechnology in medicine: moving from the bench to the bedside. Chimia. 2002; 56:520–526.

Inerot S, Heinegard D, Audell L, Olsson S-E. Articular-cartilage proteoglycans in aging and osteoarthritis. Biochem. J. 1978; 169:143–156. [PubMed: 629741]

Jarchow J, Fritz J, Anselmetti D, Calabro A, Hascall VC, Gerosa D, Berger MM, Busquets X-F. Supramolecular structure of a new family of circular proteoglycans mediating cell adhesion in sponges. J. Struct. Biol. 2000; 132:95–105. [PubMed: 11162731]

Kopesky PW, Lee H-Y, Vanderploeg EJ, Kisiday JD, Frisbie DD, Plaas AHK, Ortiz C, Grodzinsky AJ. Adult equine bone marrow stromal cells produce a cartilage-like ECM mechanically superior to animal-matched adult chondrocytes. Matrix Biol. 2010; 29:427–438. [PubMed: 20153827]

Lark MW, Bayne EK, Flanagan J, Harper CF, Hoerrner LA, Hutchinson NI, Singer II, Donatelli SA, Weidner JR, Williams HR, Mumford RA, Lohmander LS. Aggrecan degradation in human cartilage. Evidence for both matrix metalloproteinase and aggrecanase activity in normal, osteoarthritic, and rheumatoid joints. J.Clin. Invest. 1997; 100:93–106. [PubMed: 9202061]

Lee H-Y, Kopesky PW, Plaas AHK, Sandy JD, Kisiday J, Frisbie D, Grodzinsky AJ, Ortiz C. Adult bone marrow stromal cell-based tissue-engineered aggrecan exhibits ultrastructure and nanomechanical properties superior to native cartilage. Osteoarthr. Cartilage. 2010; 18:1477–1486.

Maroudas, A. Physicochemical properties of articular cartilage. Freeman, MAR., editor. Pitman, England: Adult Articular Cartilage; 1979. p. 215-290.

Maroudas A, Bayliss MT, Uchitel-Kaushansky N, Schneiderman R, Gilav E. Aggrecan turnover in human articular cartilage: use of aspartic acid racemization as a marker of molecular age. Arch. Biochem. Biophys. 1998; 350:61–71. [PubMed: 9466821]

Mercuri FA, Doege KJ, Arner EC, Pratta MA, Last K, Fosang AJ. Recombinant human aggrecan G1-G2 exhibits native binding properties and substrate specificity for matrix metalloproteinases and aggrecanase. J. Biol. Chem. 1999; 274:32387–32395. [PubMed: 10542281]

Morgelin M, Paulsson M, Hardingham TE, Heinegard D, Engel J. Cartilage proteoglycans : assembly with hyaluronate and link protein studies by electron microscopy. Biochem. J. 1988; 253:175–185. [PubMed: 3421941]

Muir, IHM. Biochemistry. Freeman, MAR., editor. Pitman Medical, Kent: Adult Articular Cartilage; 1979. p. 145-214.

Ng L, Grodzinsky AJ, Patwari P, Sandy J, Plaas A, Ortiz C. Individual cartilage aggrecan macromolecules and their constituent glycosaminoglycans visualized via atomic force microscopy. J. Struct. Biol. 2003; 143:242–257. [PubMed: 14572479]

Oike Y, Kimata K, Shinomura T, Nakazawa K, Suzuki S. Structural analysis of chick- embryo cartilage proteoglycan by selective degradation with chondroitin lyases (chondroitinases) and endo-beta-D-galactosidase (keratanase). Biochem. J. 1980; 191:193–207. [PubMed: 6781489]

Plaas AHK, West LA, Midura RJ. Keratan sulfate disaccharide composition determined by FACE analysis of keratanase II and endo-{beta}-galactosidase digestion products. Glycobiology. 2001; 11:779–790. [PubMed: 11588154]

Plaas AHK, Wong-Palms S, Roughley PJ, Midura RJ, Hascall VC. Chemical and immunological assay of the nonreducing terminal residues of chondroitin sulfate from human aggrecan. J. Biol. Chem. 1997; 272:20603–20610. [PubMed: 9252375]

Rodriguez E, Roland SK, Plaas A, Roughley PJ. The glycosaminoglycan attachment regions of human aggrecan. J. Biol. Chem. 2006; 281:18444–18450. [PubMed: 16679517]

Rosenberg L, Hellmann W, Kleinschmidt AK. Electron microscopic studies of proteoglycan aggregates from bovine articular cartilage. J. Biol. Chem. 1975; 250:1877–1883. [PubMed: 163258]

Roughley P, Martens D, Rantakokko J, Alini M, Mwale F, Antoniou J. The involvement of aggrecan polymorphism in degeneration of human intervertebral disc and articular cartilage. European Cells & Materials Journal. 2006; 11:1–7. [PubMed: 16425147]

Roughley PJ, White RJ. Age-related changes in the structure of the proteoglycan subunits from human articular cartilage. J. Biol. Chem. 1980; 255:217–224. [PubMed: 7350154]

Sandy JD, Verscharen C. Analysis of aggrecan in human knee cartilage and synovial fluid indicates that aggrecanase (ADAMTS) activity is responsible for the catabolic turnover and loss of whole aggrecan whereas other protease activity is required for C-terminal processing in vivo. Biochem. J. 2001; 358:615–626. [PubMed: 11535123]

Sandy JD, Neame PJ, Boynton RE, Flannery CR. Catabolism of aggrecan in cartilage explants. Identification of a major cleavage site within the interglobular domain. J. Biol. Chem. 1991; 266:8683–8685. [PubMed: 2026585]

Santer V, White RJ, Roughley PJ. *O*-linked oligosaccharides of human articular cartilage proteoglycan. Biochim. Biophys. Acta. 1982; 716:277–282. [PubMed: 7115751]

Stolz M, Aebi U, Stoffler D. Developing scanning probe-based nanodevices - stepping out of the laboratory into the clinic. Nanomedicine-Nanotechnology Biology And Medicine. 2007; 3:53–62.

Thyberg J. Electron microscopy of cartilage proteoglycans. Histochem. J. 1977; 9:259–266. [PubMed: 68024]

Todd BA, Rammohan J, Eppell SJ. Connecting Nanoscale Images of Proteins with Their Genetic Sequences. Biophys. J. 2003; 84:3982–3991. [PubMed: 12770903]

Tortorella MD, Liu R-Q, Burn T, Newton RC, Arner E. Characterization of human aggrecanase 2 (ADAM-TS5): substrate specificity studies and comparison with aggrecanase 1 (ADAM-TS4). Matrix Biol. 2002; 21:499–511. [PubMed: 12392761]

Verzijl N, DeGroot J, Bank RA, Bayliss MT, Bijlsma JWJ, Lafeber FPJG, Maroudas A, TeKoppele JM. Age-related accumulation of the advanced glycation endproduct pentosidine in human articular cartilage aggrecan: the use of pentosidine levels as a quantitative measure of protein turnover. Matrix Biol. 2001; 20:409–417. [PubMed: 11691581]

Wiedemann H, Paulsson M, Timpl R, Engel J, Heinegard D. Domain structure of cartilage proteoglycans revealed by rotary shadowing of intact and fragmented molecules. Biochem. J. 1984; 224:331–333. [PubMed: 6508768]

Wight, TN.; Heinegard, DK.; Hascall, VC. Proteoglycans: Structure and function. In: Hey, ED., editor. Cell biology of the extracellular matrix. New York: Plenum Press; 1991. p. 45-78.

Wilbur JL, Kumar A, Kim E, Whitesides GM. Microfabrication by microcontact printing of self-assembled monolayers. Adv. Mater. 1994; 6:600–604.

Williamson AK, Chen AC, Sah RL. Compressive properties and function-composition relationships of developing bovine articular cartilage. J. Orthop. Res. 2001; 19:1113–1121. [PubMed: 11781013]

Yasumoto T, Bird JLE, Sugimoto K, Mason RM, Bayliss MT. The G1 domain of aggrecan released from porcine articular cartilage forms stable complexes with hyaluronan/link protein. Rheumatology (Oxford). 2003; 42:336–342. [PubMed: 12595632]

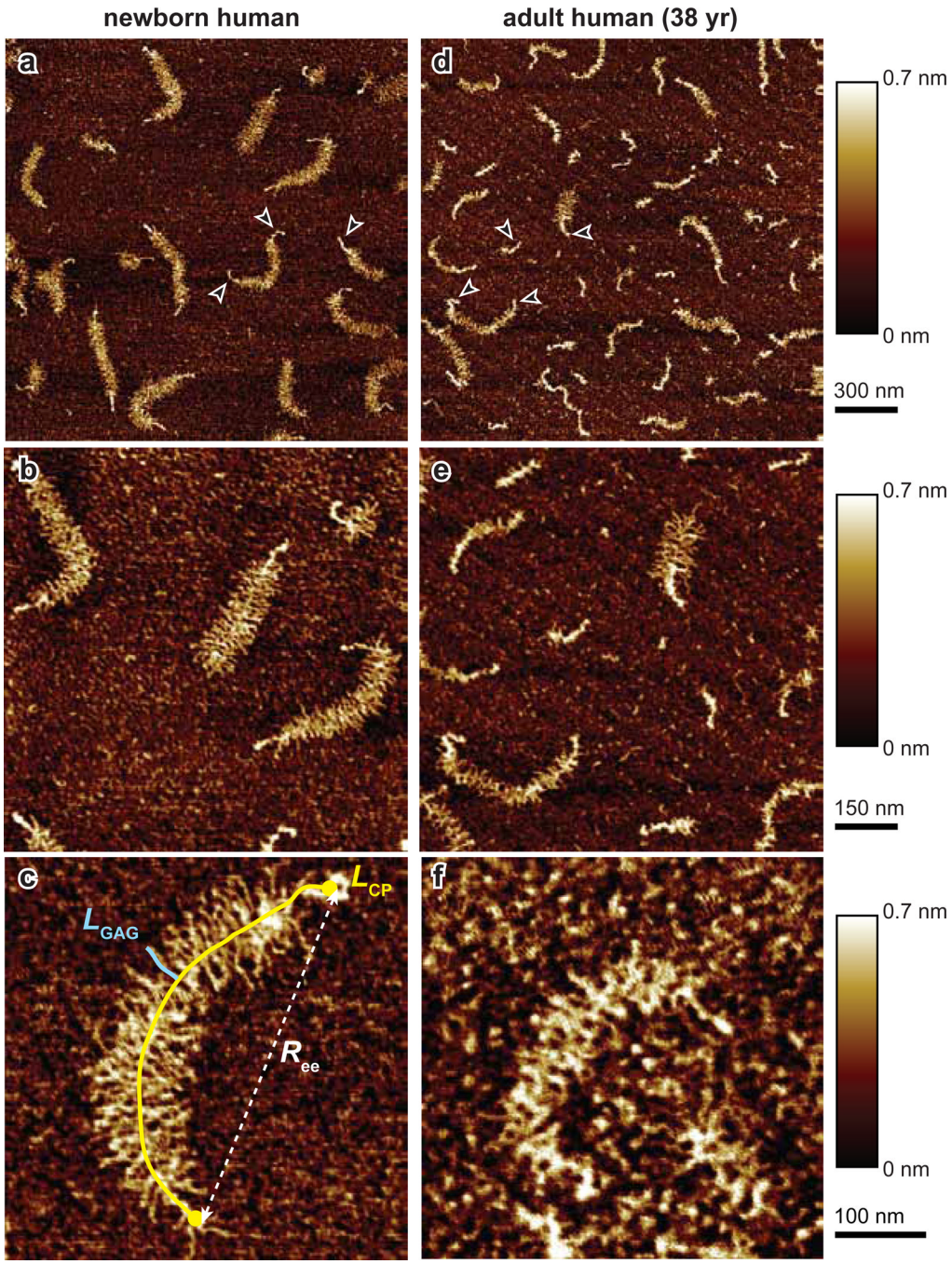

Figure 1.

Tapping mode AFM height images of (a, b, c) newborn and (d, e, f) 38-year old adult human aggrecan monomers. Globular domains are indicated by arrows (a and d). An example of core protein trace, L_{CP}, end-to-end distance, R_{ee}, and GAG chain trace, L_{GAG}, are shown in (c).

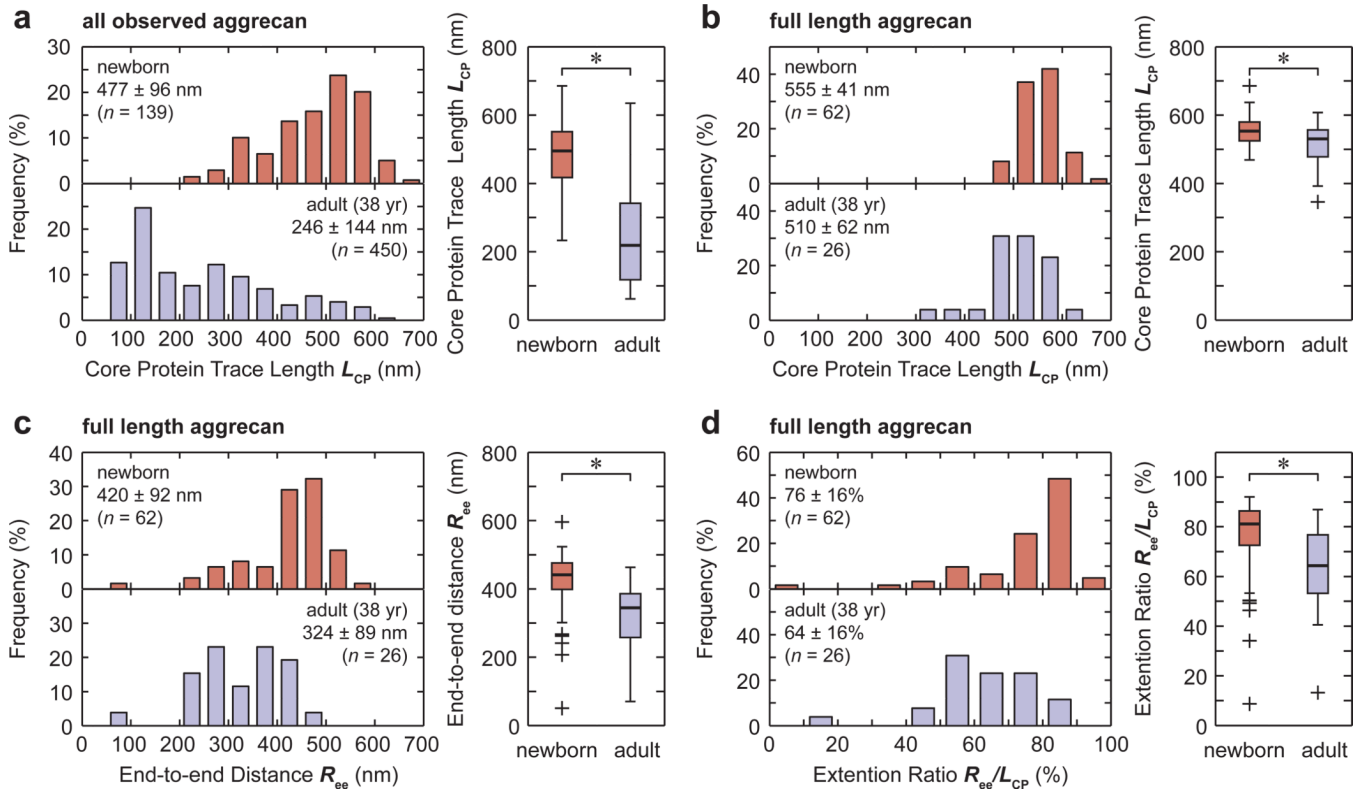

Figure 2.

Histograms and box-and-whisker plots of structural parameter distributions of newborn and 38-year-old adult human aggrecan monomer core proteins: (a) trace length, L_{CP}, of all observed aggrecan, (b) trace length, L_{CP}, of full length aggrecan, (c) end-to-end distance, R_{ee}, of full length aggrecan, and (d) extension ratio, R_{ee}/L_{CP}, of full length aggrecan. *: $p <$ 0.01 between the newborn and adult human aggrecan populations via Mann-Whitney U test.

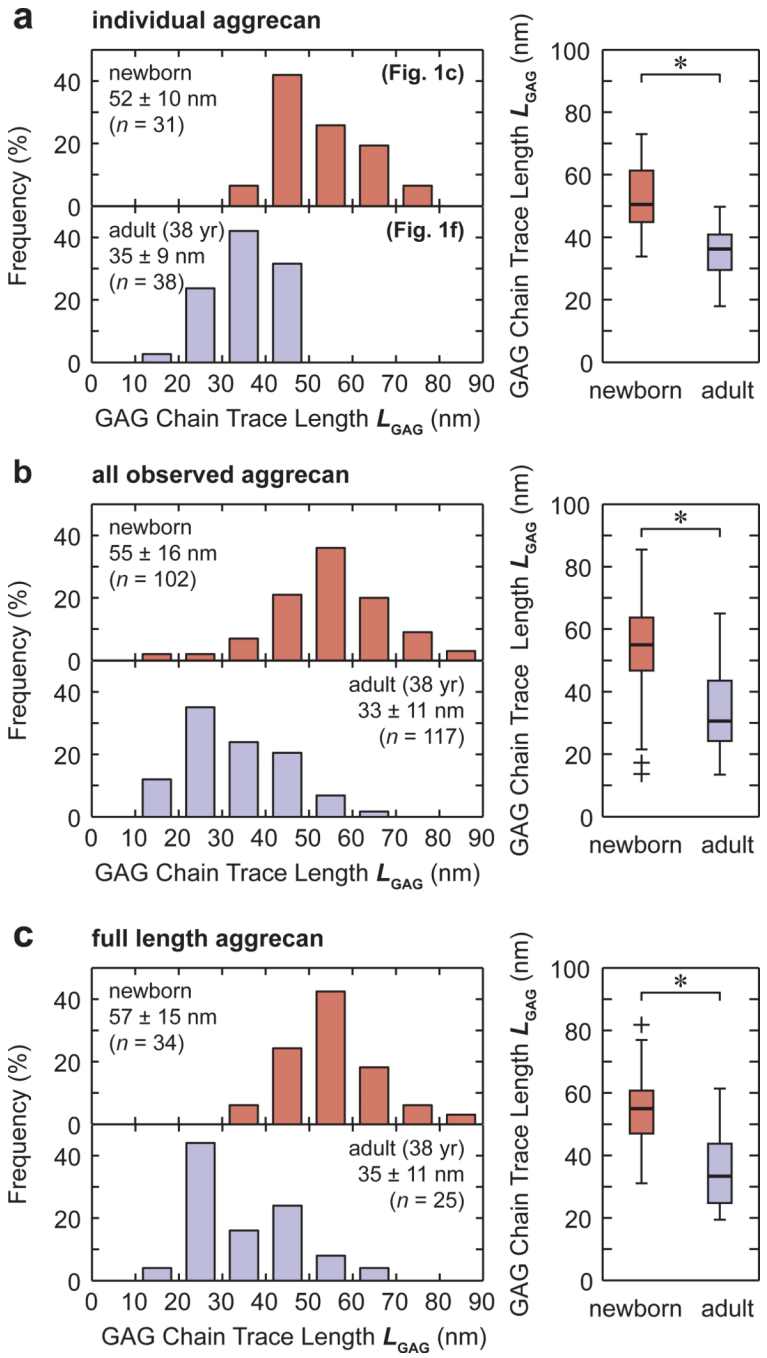

Figure 3.

Histograms and box-and-whisker plots of newborn and 38-year-old adult human aggrecan monomer GAG side chain trace length, L_{GAG}, distributions: (a) individual aggrecan, (b) all observed aggrecan, (c) full length aggrecan. *: $p < 0.0001$ between the newborn and adult human aggrecan populations via Mann-Whitney U test.

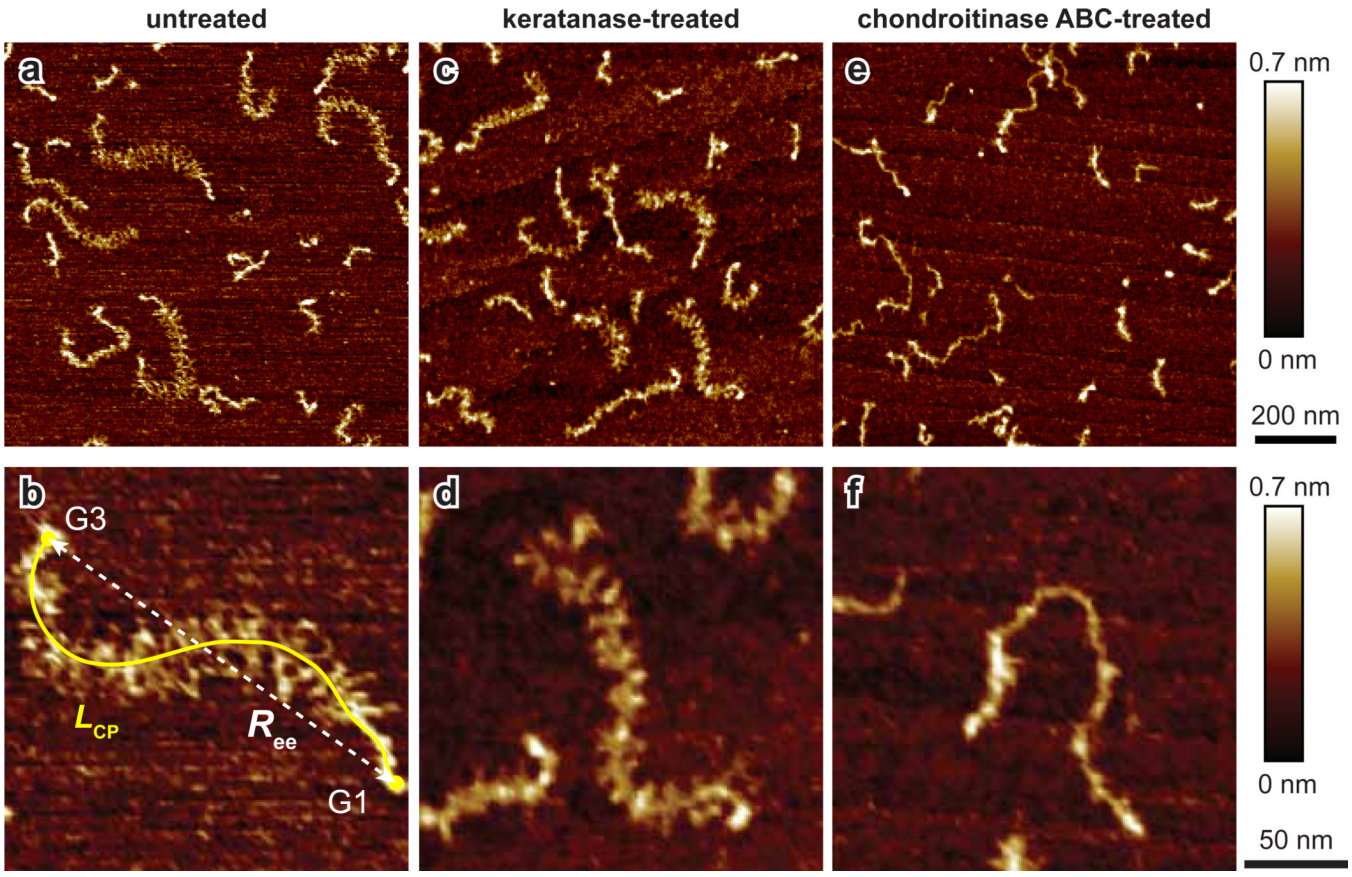

Figure 4.

Tapping mode AFM height images of (a, b) untreated, (c, d) keratanase II-treated and (e, f) chondroitinase ABC-treated 29 year old adult human aggrecan monomers. An example of core protein trace, L_{CP}, and end-to-end distance, R_{ee}, are shown in (b).

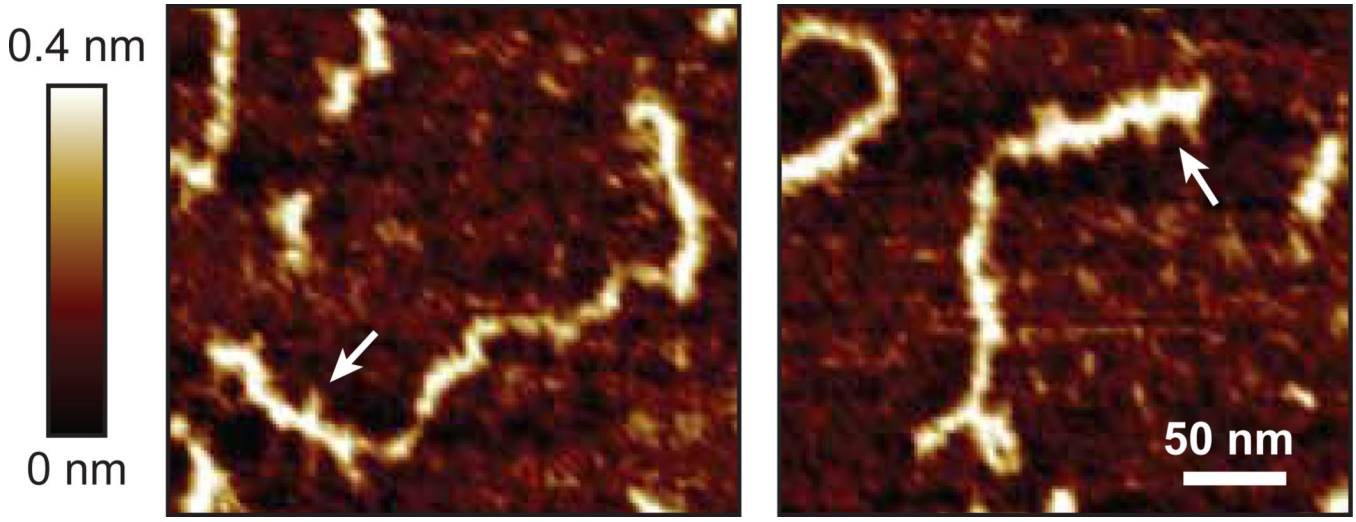

Figure 5.
Tapping mode AFM height images of chondroitinase ABC-treated aggrecan monomers. The presence of short GAG side chains, presumably KS-GAGs, are visualized near one end of the core proteins (arrows), likely within the KS-domain along the core protein.

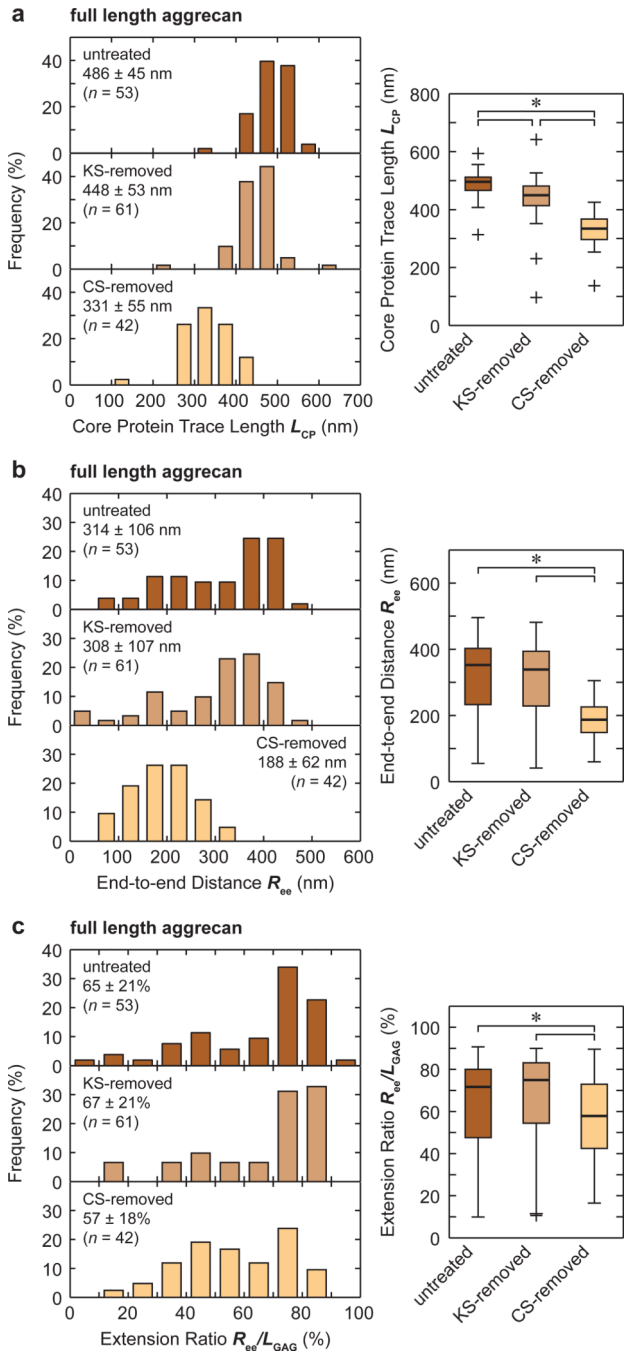

Figure 6.

Histograms and box-and-whisker plots of the structural parameter distributions of 29-year-old full length adult human aggrecan monomers: (a) core protein trace length, L_{CP}, (b) end-to-end distance, R_{ee}, and (c) extension ratio, R_{ee}/L_{CP}. Only full length aggrecan monomers with indentifiable G1 and G3 globular domains are included. *: $p < 0.05$ for each population compared with the other two populations via Mann-Whitney U test.

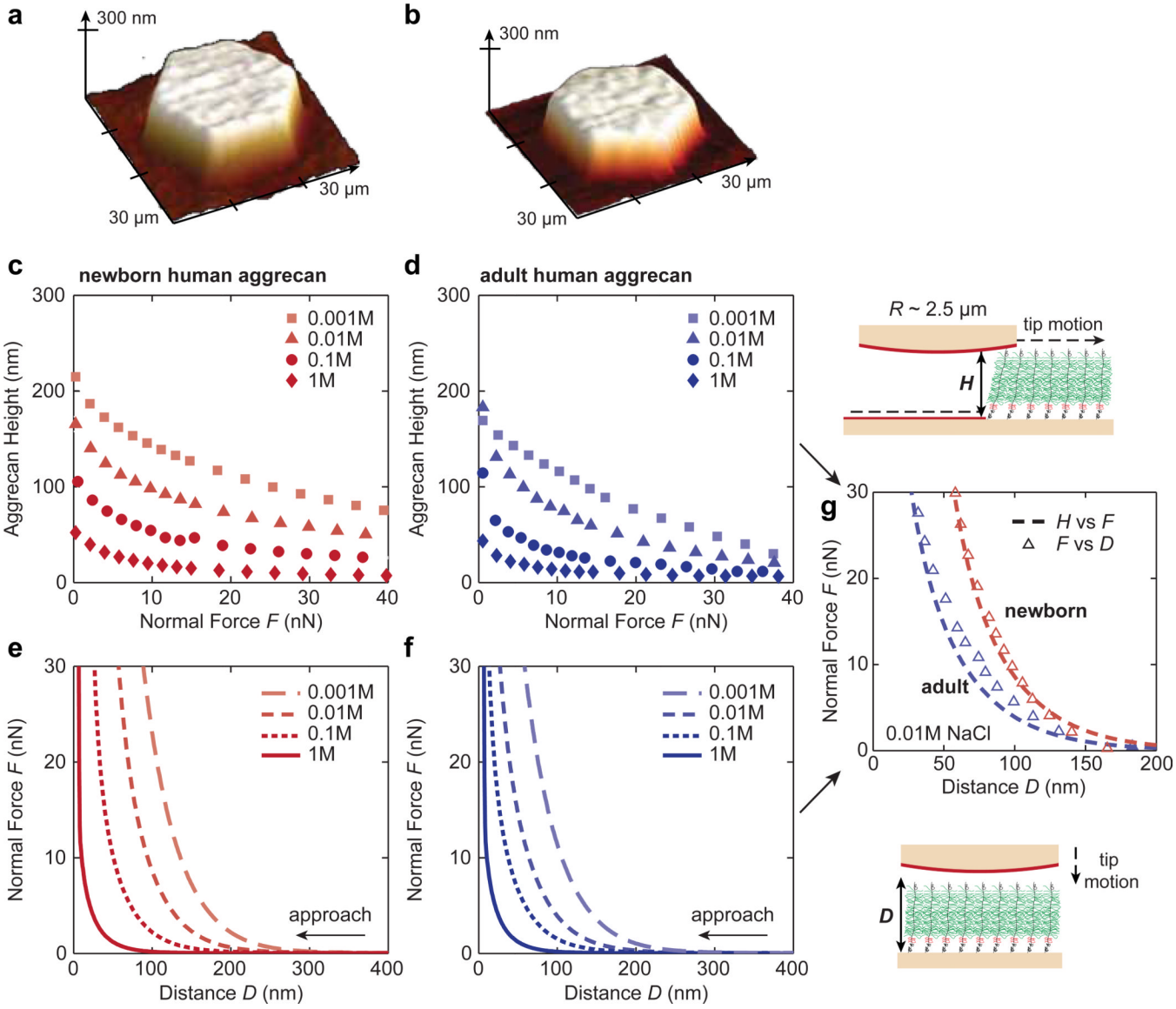

Figure 7.

(a–d) Three dimensional height images (at ~ 3 nN applied normal force) and compressed aggrecan layer height, *H*, versus applied normal force, *F*, curves of end-grafted (a,c) newborn and (b,d) adult human aggrecan layers, measured via contact mode AFM imaging on an aggrecan and hydroxyl-terminated self-assembled monolayer (OH-SAM) micro-patterned surface (top right schematic). Each data point represents the average of eight different scan locations under the same normal force, the SDs are smaller than the size of the data symbols. (e–f) Normal force, *F*, versus distance, *D*, curves of end-grafted (e) newborn and (f) adult human aggrecan layers, measured via AFM-based colloidal force spectroscopy. The probe tip approached the substrate perpendicular to the plane of the substrate (bottom right schematic). Each curve represents the average of 30 different locations on the aggrecan pattern, the SDs are smaller than the width of the data curves. (g) Comparison of the *H* versus *F* (open triangles, replotted from c and d) and *F* versus *D* (dashed lines, replotted from e and f) measurements at 0.01 M ionic strength. All the experiments were conducted in NaCl aqueous solutions at 0.001 – 1.0 M ionic strengths using a gold-coated spherical colloidal probe tip (*R* ~ 2.5 μm), functionalized with OH-SAM.

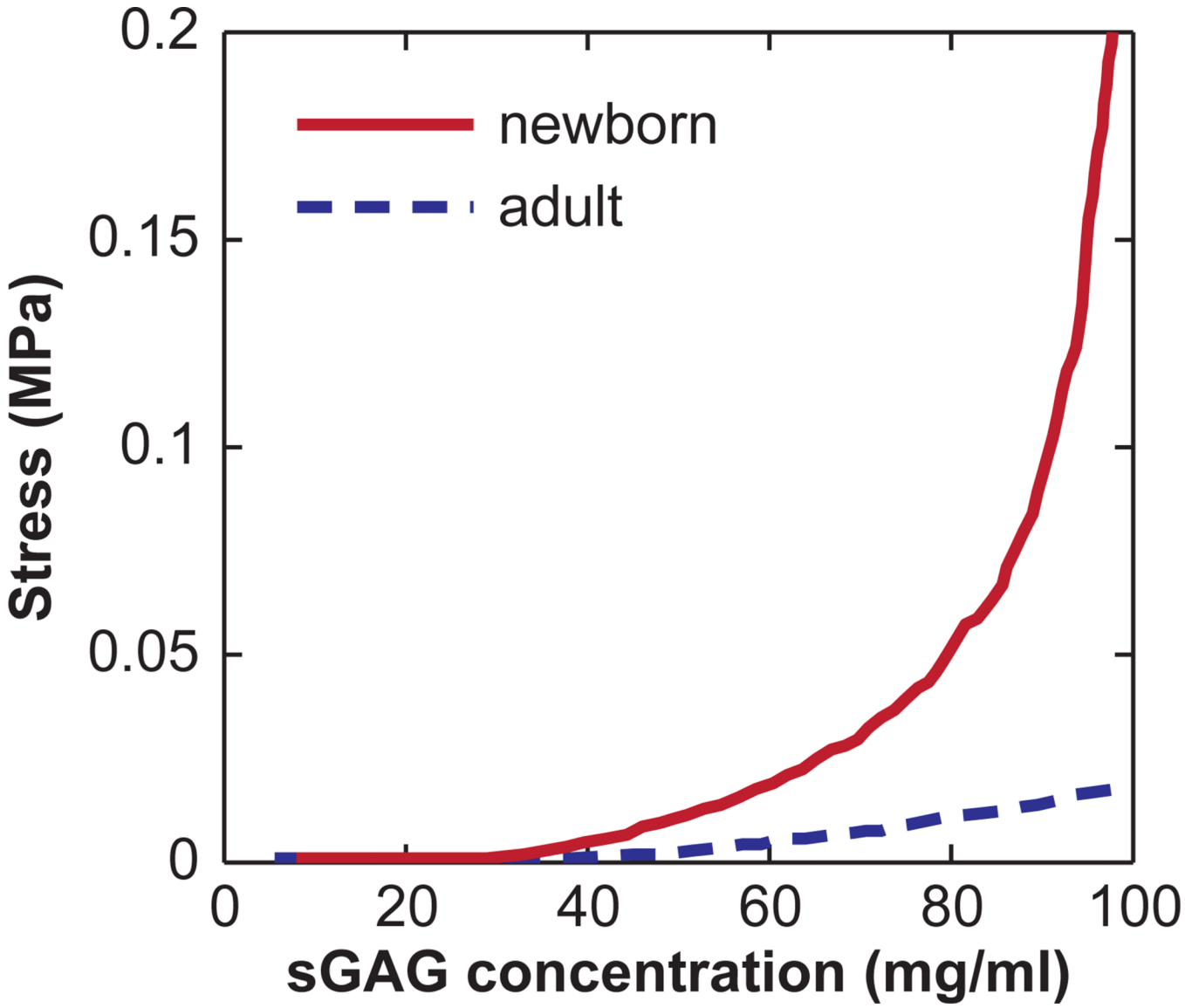

Figure 8.
Stress versus sGAG concentration curves converted from force-distance curves in Fig. 7e and f (0.1 M NaCl). Each curve is an average of 30 approaches at different locations on the aggrecan pattern. The 95% confidence intervals of each averaged curve are smaller than the width of the data curves.

Table 1

Summary of measured aggrecan structural parameters from AFM images (mean ± 95% confidence interval of means)

	all aggrecan		full length aggrecan			
	L_{CP} (nm)	*n*	L_{CP} (nm)	R_{ee} (nm)	R_{ee}/L_{CP} (%)	*n*
newborn	477 ± 16	139	554 ± 10	420 ± 23	76 ± 4%	62
38 yr-old	246 ± 13	450	510 ± 24	324 ± 35	64 ± 6%	26
29 yr-old untreated	216 ± 20	193	486 ± 12	314 ± 29	65 ± 6%	53
KS removed	207 ± 21	152	443 ± 18	304 ± 28	68 ± 5%	62
CS removed	145 ± 9	377	331 ± 17	188 ± 19	57 ± 6%	42

Table 2

Summary of measured aggrecan glycosaminoglycan (GAG) side chain trace lengths from AFM images of untreated aggrecan (mean ± 95% confidence interval of means)

	all aggrecan		full length aggrecan		individual aggrecan	
	L_{GAG} (nm)	*n*	L_{GAG} (nm)	*n*	L_{GAG} (nm)	*n*
newborn	55 ± 3	102	57 ± 5	34	52 ± 4	31
38 yr-old	33 ± 2	117	35 ± 5	25	35 ± 3	38
29 yr-old	29 ± 1	127	32 ± 3	29	--	